CHEMNANOMAT

CHEMISTRY OF NANOMATERIALS FOR ENERGY, BIOLOGY AND MORE

www.chemnanomat.org

Accepted Article

Title: Strategies to Build High-Rate Cathode Materials for Na-Ion Batteries

Authors: Wei-Jun Lv, Zhigao Huang, Ya-Xia Yin, Hu-Rong Yao, Hai-Liang Zhu, and Yu-Guo Guo

To be cited as: *ChemNanoMat* 10.1002/cnma.201900254

Link to VoR: http://dx.doi.org/10.1002/cnma.201900254

A Journal of

ACES Asian Chemical Editorial Society

A sister journal of **Chemistry – An Asian Journal** and **Asian Journal of Organic Chemistry**

WILEY-VCH

10.1002/cnma.201900254
WILEY-VCH

FOCUS REVIEW

Strategies to Build High-Rate Cathode Materials for Na-Ion Batteries

Wei-Jun Lv,[a],[c] Zhigao Huang,[a],[c] Ya-Xia Yin,[b],[d] Hu-Rong Yao,*[a],[b],[c] Hai-Liang Zhu*[b] and Yu-Guo Guo*[b],[d]

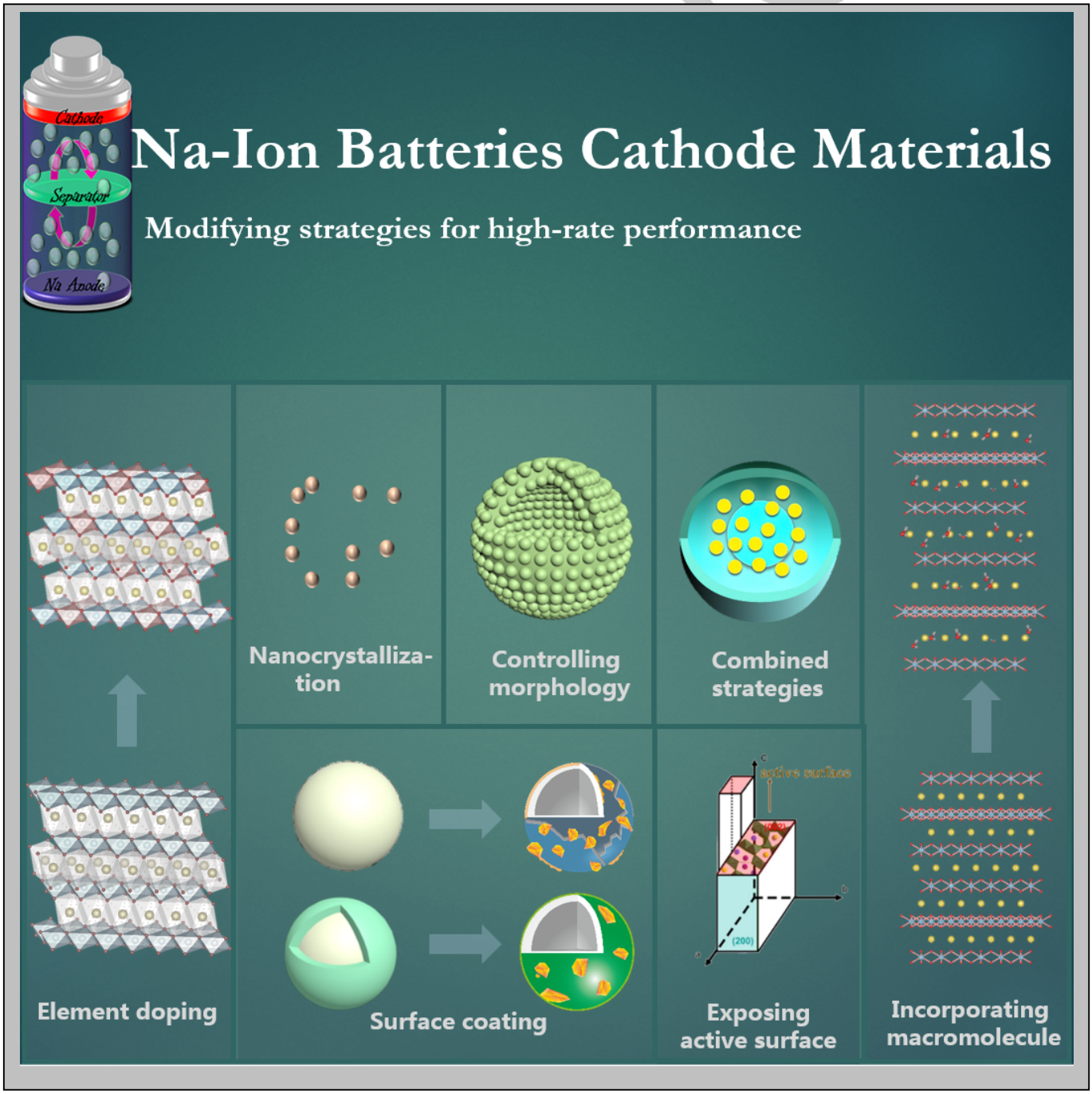

Abstract: The development of cathode materials for Na-ion batteries (NIBs) have received abundance lessons from the previous research on Li-ion batteries (LIBs) due to the similar physicochemical properties between Na and Li. However, the exploitation of high-rate NIB cathodes has faced greater difficulty compared to the Li counterparts because of a larger ionic radius of Na. A lot of attempts on optimization of composition and structure have been made to address this issue, which achieved great progress and considerable attention in recent years. Herein, a systemic review on the latest researches of high-rate cathode materials for NIBs is presented. In addition, a comprehensive analysis on specific reasons hindering the kinetic performance is also discussed, expecting to deepen the understanding on mechanism behind rate performance and provide a new avenue of designing high-performance NIBs.

1. Introduction

Nowadays, the exploitation of highly efficient and clean energy storage systems (ESS) become more and more important for human society due to the tremendous pressure of global warming and environmental crisis.[1–3] Among various ESS, LIBs have attracted considerable attention and gained successful commercialization because of its high energy density and power density.[4,5] However, the rapid development of portable electronics and electric vehicles puts forwards higher demands to LIBs, which forms a sharp contradiction with rarity of Li resources. The increasing market and cost consideration drive the exploitation of an optimized alternative for LIBs. In this context, NIBs show great potential and received extensive studies owing to Na similar physicochemical properties to Li, low cost benefiting from the abundance of Na and compatibility of anodic Al current collector.[6–9]

Considering the direct effect of cathode performance on cell properties, a lot of attempts have been made to look for positive electrode materials with excellent electrochemical performances in terms of capacity, voltage, cycling stability and rate capability.[10–15] In the fast-paced modern society, rate capability is becoming more and more important as the demand increase for fast-charging capability in portable electronics and electronic vehicles. Unfortunately, for the transition from LIBs to NIBs, exploitation of high-rate cathode materials is hampered by greater difficulty originating from the larger ionic radius of Na^+ (1.02 Å) than 0.76 Å of Li^+ and the difference of thermodynamic phase in some materials (e.g. maricite of $NaFePO_4$ and olivine of $LiFePO_4$).[16] Extensive efforts have been made to understand the mechanism of sluggish kinetic performance and try to design high-rate cathode materials by tuning composition and structure.

In this review, we classify the influencing factors on kinetic performance into four parameters in order to grasp deep insights for understanding kinetic mechanisms: electronic conductivity, ionic conductivity, side reactions and phase transitions. Also, we pay attention to recent research progress on corresponding strategies modifying kinetics of cathode materials for NIBs and classify the strategies into nanocrystallization, surface coating, element doping, controlling morphology, exposing active surface, incorporating macromolecule and combined method. In addition, we analysis the working mechanism of each strategy and try to provide effective method to further improve the kinetic performance. Based on the systematic analysis and understanding extracted from recent progress, the new research direction will be opened up for designing cathode materials with excellent rate performance.

Wei-Jun Lv is currently a master graduate student in College of Physics and Energy at Fujian Normal University. He received his Bachelor degree from Fujian Normal University in 2018. His research focuses on electrode materials for rechargeable Na-ion batteries.

Hu-Rong Yao is a lecturer at Fujian Normal University. She received her PHD degree in Physical Chemistry under the supervision of Pro. Yu-Guo Guo from Institute of Chemistry, Chinese Academy of Sciences (ICCAS) in 2017. Her research focuses on advanced electrode materials for rechargeable batteries.

[a] Mr. Wei-Jun Lv, Prof. Zhigao Huang, Dr. Hu-Rong Yao
Fujian Provincial Key Laboratory of Quantum Manipulation and New Energy Materials College of Physics and Energy, Fujian Normal University
Fuzhou 350117, China

[b] Dr. Hu-Rong Yao, Prof. Ya-Xia Yin, Dr. Hai-Liang Zhu, Prof. Yu-Guo Guo
CAS Key Laboratory of Molecular Nanostructure and Nanotechnology, CAS Research/Education Center for Excellence in Molecular Sciences, Beijing National Laboratory for Molecular Sciences (BNLMS)
Institute of Chemistry, Chinese Academy of Sciences (CAS)
Beijing 100190, P. R. China

[c] Mr. Wei-Jun Lv, Prof. Zhigao Huang, Dr. Hu-Rong Yao
Fujian Provincial Collaborative Innovation Center for Optoelectronic Semiconductors and Efficient Devices
Xiamen, 361005, China

[d] Prof. Ya-Xia Yin, Prof. Yu-Guo Guo
University of Chinese Academy of Sciences
Beijing 100049, China

E-mail: yaoyao@fjnu.edu.cn, ygguo@iccas.ac.cn

Yu-Guo Guo is a Professor of Chemistry at ICCAS. He received his PhD in Physical Chemistry from ICCAS in 2004. He worked at the Max Planck Institute for Solid State Research in Stuttgart (Germany) first as a Guest Scientist and then a Staff Scientist from 2004 to 2007. He joined ICCAS as a full professor in 2007. His research focuses on nanostructured energy materials and electrochemical energy storage devices.

2. Influencing Factors

Based on a "rocking-chair" working principle, Na^+/electrons deintercalate from cathode and pass though electrolyte/external circuit and then insert into anode upon charging, and vice versa upon discharging. Therefore, from the cathode perspective, the factors influencing electrons and ions transport kinetics exhibit an important impact on the rate performances, which can be divided into following four aspects: electronic conductivity, ionic conductivity, side reactions, phase transitions.

2.1 Electronic conductivity

Because the electrochemical process of cells relies on the shuttle of Na^+ and electron between cathode and anode to ensure charge balance, the electronic conductivity is a key indicator for the rate performance of host materials. There are two different mechanisms describing the electron conductive principles in cathodes. Materials like $NaCoO_2$ are metallic conductors at certain Na concentration,[17] resulting to excellent electronic conductivity. In compared, the electron transport in $Na_2Fe_2(SO_4)_3$ proceeds by polaron hopping mechanism,[18] and the localized hopping usually leads to a poor chemical diffusion coefficient.

With the help of density functional theory, it is realizable to quantitatively calculate band gap of materials and analyze electronic conductivity. Polyanionic compounds and prussian blue analogues (PBAs) usually exhibit low electron conductivity due to their insulating characters or structural defects. $Na_3V_2(PO_4)_3$ is predicted to have poor electronic conductivity owing to its large band gap of 1.735 eV, might originating from the high electron affinity of V atom and the existence of distorted VO_6 octahedral units. Furthermore, Al-doping is suggested to decrease the band gap due to the low electron affinity of Al atom (Figure 1). [19] In PBAs, the presence of $Fe(CN)_6$ vacancies may destroy electronic conduction along Fe-C≡N-M frame-work structure, thus significantly limiting the rate performance.[2,20] Based on the above reasons, both coating by materials with high electronic conductivity and defect chemistry are widely used to mitigate the limitation, which will be discussed in the following sections in detail.

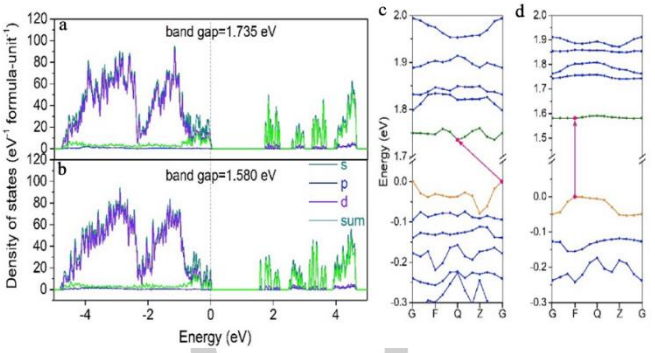

Figure 1. a) Total density of states of $Na_3V_2(PO_4)_3$, b) and $Na_3V_{1.75}Al_{0.25}(PO_4)_3$. The vertical line at zero point represents the Fermi level. Band structure of c) $Na_3V_2(PO_4)_3$, and d) $Na_3V_{1.75}Al_{0.25}(PO_4)_3$. Reproduced with permission.[19] Copyright 2018, Elsevier.

2.2 Ionic conductivity

Compared to the electron conduction, diffusion of Na^+ in cathode materials is more difficult owing to its heavier weight and larger radius. Therefore, Na^+ diffusion coefficient is a very important parameter for power density of cells, which is closely related to the dimension, length, space and topology of Na^+ diffusion channel.

2.2.1 Diffusion dimensional

According to the difference on dimension of diffusion channel, the active cathodes for NIBs can be divided to three types: 1D, 2D and 3D (Figure 2).[21–24] Theoretically, a multiple dimensional ion diffusion channel corresponds to higher ion diffusion coefficient, which also be widely proved by experiments. For example, the olivine $NaFePO_4$, synthesized via chemical or electrochemical displacement methods from olivine $LiFePO_4$,[10] exhibits a low ionic conductivity owing to its 1D ion diffusion channel. In contrast, $Na_3V_2(PO_4)_3$, a typical NASCION-type cathode of NIBs,[25–27] provides 3D channels for Na^+ insertion/extraction, resulting in an excellent ionic conductivity. Similarly, the 3D ions diffusion channels and open crystal structure in PBAs are conducive to the migration of Na^+ in host structure and could effectively accommodate the lattice volume change, promising an attractive rate performance. However, the presence of coordinated water in the crystal frame-work structure of PBAs,[28,29] originating from the imperfect synthetic method, always block the active diffusion pathway, severely deteriorating the electrochemical performances.

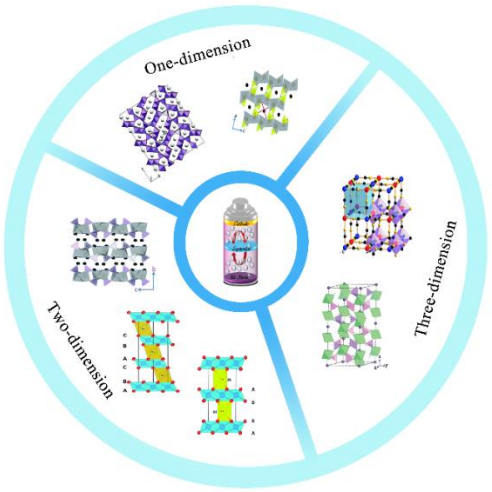

Figure 2. Structural schematic illustrations of several typical cathode materials for NIBs, which contains different dimension ion diffusion channels. olivine-type $NaFePO_4$, and $Na_{0.44}MnO_2$, both contains one-dimension ion diffusion channels. Reproduced with permission.[30] Copyright 2013, Royal Society of Chemistry, Reproduced with permission.[14] Copyright 2007, American Chemical Society, respectively. Na_2FePO_4F, O3-type, and P2-type layered oxides, all contains two-dimension ion diffusion channels. Reproduced with permission.[30] Copyright 2013, Royal Society of Chemistry. Reproduced with permission.[7] Copyright 2013, Royal Society of Chemistry. respectively. $Na_3V_2(PO_4)_3$, Prussian blue analogue, both contains three-dimension ion diffusion channels. Reproduced with permission.[31] Copyright 2014, Royal Society of Chemistry. Reproduced with permission.[11] Copyright 2012, Royal Society of Chemistry, respectively. (From left to right.)

2.2.2 Diffusion length

From ion diffusion perspective, the mean diffusion time of Na^+ (τ) is related to diffusion coefficient (D) and diffusion length (L) as the following formula:

$$\tau = L^2/2D$$

It is obvious that kinetics can be accelerated by increase of D or decrease of L.[32] Compared to modification on bulk structure with the aim of increasing D, the decrease of L could be easier to realize by nanocrystallization, which is excellently effective for the improvement of rate performance due to the square law between τ and L. For materials with 1D ion diffusion channel, the strategy of reducing diffusion length is extraordinarily valid because long diffusion length always results in the blockage of active pathway for Na^+ insertion/extraction.

2.2.3 Diffusion space

Though substantial efforts have been devoted to decrease diffusion length, the diffusion coefficient D is never changed, which is an important intrinsic parameter for rate performance of materials. Based on lattice gas model, the diffusion coefficient can be calculated from

$$D = \nu_0 l^2 \exp(-\frac{E_a}{K_B T})$$

where ν_0 is ion vibration frequency, l is hopping distance, E_a is the migration energy barrier of Na^+, K_B and T are Boltzmann constant and absolute temperature, respectively. From the point of structure design, E_a is a key indicator for kinetic performance, which is influenced by two major structure factors: space and topology of diffusion channel, discussed in this and next section respectively.

P2- and O3-type layered oxide cathodes have similar layered structure, in which Na^+ intercalate into the interlayer of edge sharing TmO_6 (Tm: transition metal) octahedral layers. In spite of the similar structure, P2-mateials always exhibit better rate performance than O3-structure owing to the larger space for prismatic site of Na^+ in P2-structure.[33] Intuitively, incorporating macromolecule into diffusion pathway is effective to rationally enlarge channel space. Besides, it is worth noting that nanocrystallization has also been wildly used to enlarge the space of diffusion channel upon the ratio increase of surface phase.

2.2.4 Diffusion topology

Beside the space of diffusion channel, channel topology need to offer highly accessible ion diffusion pathway for designing high-rate cathodes. According to results of the first principle calculations, diffusion barrier of Na^+ in P2-materials is lower than P3-type due to the existence of multi Na vacancies, in spite of their similar P-type structure.[34] The topology arrange of Na^+/vacancies in the Na layer is also highly connected to the Na^+ diffusion, which frequently occurs in the materials with ionic ordering and charge ordering.[35] The Na^+/vacancy ordering leads to multi voltage plateaus during electrochemical process, resulting in a negative effect on the rate performance. From the perspective of designing intrinsic structure, element doping is the most common method to modify the topology structure with the advantages of scalable, low-cost.

2.3 Side reactions

The side reactions between the electrolyte and cathode are responsible for some part of poor rate performance. Upon charged to high voltage, the electrolyte is prone to decompose and the decomposition further corrodes electrode materials with the emergence of side reactants, which is harmful to rate performance.[22,36,37] Jo et al. had compared bare P2-type $Na_{2/3}[Ni_{1/3}Mn_{2/3}]O_2$ and $NaPO_3$-coated $Na_{2/3}[Ni_{1/3}Mn_{2/3}]O_2$ after cycling 50 times, and found that a larger amount of HF and H_2O are existed on the particle surface of bare-$Na_{2/3}[Ni_{1/3}Mn_{2/3}]O_2$ because of the decomposition of electrolyte,[38] and the dissolved metal ions are oxidized at cathode surface, further forming passive layers containing NaF, NiO, NiF, MnF (Figure 3a-3b). Presence of these insulating substance and excessive HF would lead to remarkable decrease of ionic/electronic conductivity and corrosion of electrode materials, resulting in a poor cyclic stability and unsatisfactory rate performance.

2.4 Phase Transitions

Compared to solid-solution mechanism, the phase transition reactions during Na^+ insertion/extraction is detrimental for rate performance, originating from their slow process of nucleation

10.1002/cnma.201900254

and phase interface migration.[39] Meanwhile, the rearrangement of crystal structure during phase transitions need additional energy consumption accompanied by low energy conversion efficiency, further resulting in large voltage polarization and poor rate performance. In addition, phase transitions are usually accompanied with large volume change and collapse of bulk structure, leading to poor electrochemical properties. The effect of phase transitions on rate performance can be confirm by the property difference of two major subjects of layered oxide cathode: P2- and O3-materials. Generally, the O3-type cathode materials suffer from more complex phase transitions than P2-compounds. The phase transition O3-O′3-P3-P′3 often occurs upon charging of O3-materials, where P2 materials generally retain original structure or undergo a P2-O2 transition upon charged above 4.0 V owing to the great structure difference between P2 and P3/O3 phase. For instance, the O3-$NaNi_{0.5}Mn_{0.5}O_2$ undergoes $O3_{hex}$-$O3'_{mon}$-$P3_{hex}$-$P3'_{mo}$-$P3''_{hex}$ phase transitions during Na^+ extracting process,[12] while the P2-$Na_{2/3}Ni_{1/3}Mn_{2/3}O_2$ only suffer from a phase transition from P2 to O2.[40] Based on the above reasons, P2 cathodes generally promise better rate performance compared to O3 phases.

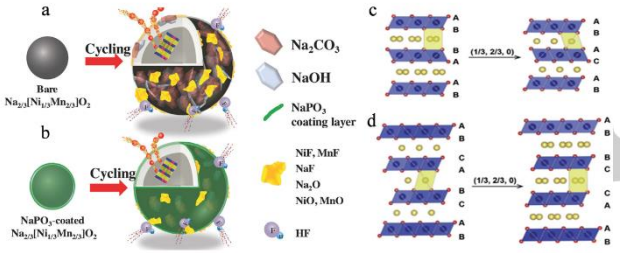

Figure 3. Schematic illustration of by-products at the surface of a) bare-$Na_{2/3}Ni_{1/3}Mn_{2/3}O_2$, and b) $NaPO_3$-coated $Na_{2/3}Ni_{1/3}Mn_{2/3}O_2$ (after cycling 50 times). Reproduced with permission.[38] Copyright 2018, Wiley-VCH. Schematic illustration of c) P2-O2 phase evolutions, and d) O3-P3 phase evolutions during Na insertion/extraction. Reproduced with permission.[39] Copyright 2017, Wiley-VCH.

3. Strategies

The multi influencing factors that bring the complexity of mechanism on rate performance also bring various modifying strategies to improve kinetics. In order to stable the capacities at high rate, considerable efforts have been made on improving the battery electrochemistry with ingenious structure/component design on electrode materials, electrolyte, separators and current collectors. From cathode perspective, the modifying mechanism mainly focus on tuning the component, improving activity, suppressing side reaction and phase transitions. The following sections will discuss the recent advances and analyze corresponding mechanism of these strategies, which can be divided into five parts according to specific method: nanocrystallization, surface coating, element doping, controlling morphology, Incorporating macromolecule, and combined strategies.

3.1 Nanocrystallization

The raising of nanotechnology has brought a new promising prospect to LIBs, which rapidly improve the electrochemical activity.[1,41] Yao et al. systematically summarized the effects of particle size of electrode materials on electrochemical properties of LIBs from the perspectives of kinetics, thermodynamics and Li storage mechanism.[32] Benefiting from the similarity between Na^+ and Li^+, the improvement in LIBs can provide a great guidance for designing high-performance cathodes for NIBs with the help of nanotechnology.

Intuitively, nanocrystallization can reduce Na^+ diffusion path and decrease the mean diffusion time and then improve the rate performance. Meanwhile, the bigger specific surface area of nano-sized materials also increases contact area between electrode material and electrolyte, promoting a higher reactivity and smaller polarization during sodiation/desodiation. M. D'Arienzo et al. studied the electrochemical properties of P2-$Na_{0.71}CoO_2$ with different morphologies, and found that particle size has a great influence on its electrochemical performance. The sample with small particle size exhibits higher specific capacity and better rate performance due to the short diffusion distance of Na ions.[42] $Na_4Mn_9O_{18}$ synthesized with polymer-pyrolysis method (Figure 4a) with a quite uniform nanowire structure delivers an optimized rate performance based on the increase of electrode/electrolyte contact area and decrease of ion diffusion distance (Figure 4b).[43] On the contrary, $Na_3V_2(PO_4)_3$ of large particles size obtained by one-step solid state reaction (Figure 4c) exhibits an unsatisfied rate performance (Figure 4d) with serious particle aggregation.[44] It is worth reminding that nanoparticles usually suffer from self-aggregation owing to the high surface energy, which seriously weaken the modifying effect.[45] Large of efforts have been made to suppress the phenomenon. Kalluri et al. prepared stable hierarchical P2-$Na_{2/3}Fe_{1/2}Mn_{1/2}O_2$ nanofibers by electrospinning, and the hierarchical structure effectively alleviate the disgusting self-aggregate because arrangement of nanoparticles is orderly distributed along the direction of fiber growth (Figure 4e).[46] The advantage leads to a remarkable rate performance than unordered nanoparticles (Figure 4f). In addition, some other methods, such as ball milling[47] and spray pyrolysis,[48] can also synthesize orderly distributed nanoparticles. For example, Rafael Klee et al. prepared $Na_3V_2(PO_4)_3$ by a ball milling assisted method, which exhibits an improved rate performance. The improvement can be ascribed to a more homogeneous distribution and the reduction of size of primary particles.[47]

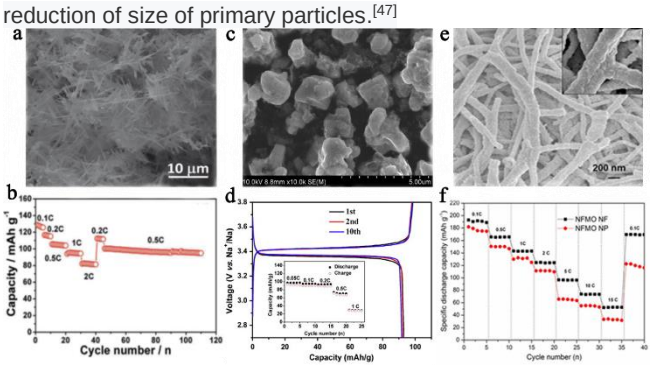

Figure 4. a) SEM image and b) rate performance of $Na_4Mn_9O_{18}$ with a quite uniform nanowire structure. Reproduced with permission.[49] Copyright 2011,

Wiley-VCH. c) SEM image and d) Charge/discharge profiles for $Na_3V_2(PO_4)_3$ with large particles. Inset is the rate performance. Reproduced with permission.[44] Copyright 2011, Elsevier. e) SEM image (inset: high-resolution image) and f) rate performance of $Na_{2/3}Fe_{1/2}Mn_{1/2}O_2$ nanofibers and $Na_{2/3}Fe_{1/2}Mn_{1/2}O_2$ nanoparticles. Reproduced with permission.[46] Copyright 2014, American Chemical Society.

3.2 Surface coating

As the increase of specific surface area with nanocrystallization, the unsatisfying side reaction is also aggravated. In this case, substantial efforts have been devoted to protect the active surface from attack of electrolyte, in which surface coating is a common strategy and has been confirmed to be a useful method. The mechanisms of surface coating on improvement of electrochemical performances include: (1) improving electron/ion transfer at the surface of active materials via coating a surface phase with high electronic/ionic conductivity; (2) forming a protective layer at electrode surface to reduce the dissolution of active materials; (3) alleviating side reaction to suppress the generation of impurities with corrosivity or poor conductivity.

To date, the materials used as coating layer mainly include carbon materials,[44,50–52] metal oxides,[22] conducting polymer,[53] and so on. Liu et al. prepared Al_2O_3 coated P2-$Na_{2/3}Ni_{1/3}Mn_{2/3}O_2$ by simple wet chemistry method, which reduces the direct contact between electrode and electrolyte and alleviates side reaction.[22] Furthermore, surface carbon coating can form a mixed conductive network for ions and electrons transport. For $Na_3V_2(PO_4)_3$/C made by hydrothermal assisted sol–gel method, the uniform surface carbon coating significantly reduces particle agglomeration, and also enhance the diffusion rate of both electrons and ions, thus making a remarkable cyclic stability and rate capability.[54] Besides, Li et al. successfully synthesized $Na_{1+x}MnFe(CN)_6$ cathode with an ClO_4-doped polypyrrole coating layer, exhibiting an amazing rate performance.[53] The existence of coating layer not only enhance the electronic conductivity, but also alleviates the dissolution of Mn in electrolyte, which promote rate and cycling performances.

3.3 Element doping

Element doping is a common method used to improve kinetics of materials because of its simple synthesis process and modifying mechanism on intrinsic component compared to nanocrystallization and surface coating. The various mechanisms of element doping on improvement of rate performance of cathode materials for NIBs is largely reported recently.[55–57]

Li et al. investigated the effect of Mg^{2+} substituting V^{3+} in $Na_3V_2(PO_4)_3$, a shorter length of V–O and P–O bonds in $Na_3V_{1.95}Mg_{0.05}(PO_4)_3$ than that of $Na_3V_2(PO_4)_3$, promising an optimized crystal structure and expanded Na^+ diffusion channels.[58] Meanwhile, the electronic conductivity is also improved by Mg substitution. The above optimizations result in a significant improvement in rate performance of $Na_3V_2(PO_4)_3$ (Figure 5a-5c). Also, element doping is effective for enhancing the structural stability. Ma et al. replaced Mn in $Na_2MnFe(CN)_6$ with inactive Ni, which could balance the structural disruption caused by the redox reaction of Mn^{2+}/Mn^{3+}, thus enhancing the rate and cycle performances. Then, element doping can inhibit the disgusting phase transitions, which is demonstrated by numerous studies. Wang et al. substituted Mn^{4+} in $NaNi_{0.5}Mn_{0.5}O_2$ by Ti^{4+} considering their similar ionic radius and same valence state.[57] Ti-doped material effectively inhibits the glide of transition metal layer upon sodiation/desodiation and exhibits only a highly reversible phase transition from O3 to P3 (Figure 5d), with a dramatic comparison to the four phase transitions of original $NaNi_{0.5}Mn_{0.5}O_2$. Similar effect has also been exhibited in Cu-doped $Na_{0.67}Ni_{0.1}Cu_{0.2}Mn_{0.7}O_2$,[59] Ca-doped $Na_{5/8}Ca_{1/24}CoO_2$,[60,61] Li and Fe co-doped $Na[Li_{0.05}(Ni_{0.25}Fe_{0.25}Mn_{0.5})_{0.95}]O_2$.[62] Another major role of element doping in layered oxides cathode materials is to modulate the interlayer spacing and suppress Na^+/vacancy ordering.[35,63,64] It is known that P2-type cathodes have a larger Na layer spacing compared to O3-materials, which can tolerate lattice distortion caused by the change of O-O bond length. Then, the larger Na layer spacing can effectively inhibit the migration of transition metal ions to alkali metal layers during charging and maintain the original structure. The other hand, enhancement of disordering in transition metal ions obtained by introduction of foreign ions is beneficial for suppression of Na^+/vacancy ordering, a main reason for the multi voltage plateaus in electrochemical curves of P2-materials. Yue et al. found that Ni and Mg co-doped $Na_{0.67}Ni_{0.1}Mn_{0.8}Mg_{0.1}O_2$ not only expand Na interlayer spacing, but also destroy Na^+/vacancy ordering, thus excellently enhancing the Na^+ diffusion rate.[63]

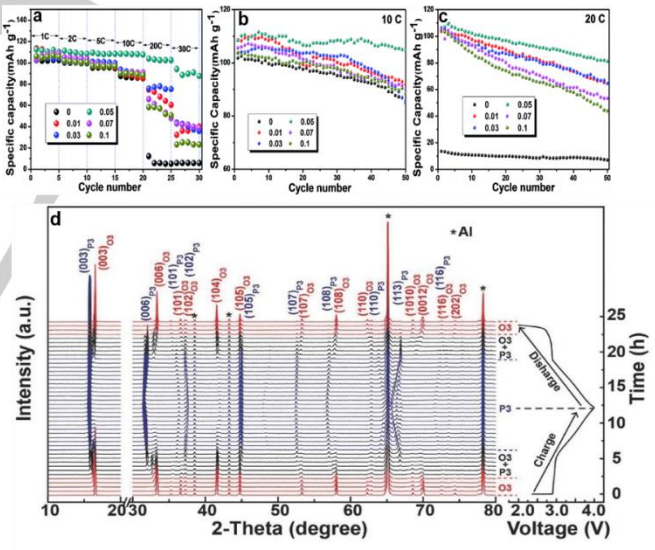

Figure 5. a) Rate performance of $Na_3V_{2-x}Mg_x(PO_4)_3$/C. Cycling stability of $Na_3V_{2-x}Mg_x(PO_4)_3$/C at b) 10 C and c) 20 C. Reproduced with permission.[58] Copyright 2015, Royal Society of Chemistry. d) In situ XRD patterns collected during the first charge/discharge of $Na/NaNi_{0.5}Mn_{0.2}Ti_{0.3}O_2$ cell under a current rate of 0.05C at voltage range between 2 and 4 V. Reproduced with permission.[57] Copyright 2017, Wiley-VCH.

3.4 Controlling morphology

The researches on electrode materials found that morphology of particles is also a key factor for their rate performance. Su et al. prepared the V_2O_5 hollow nanospheres through a template-free polyol-induced solvothermal process (Figure 6a.), and found that

the unique structure of hollow nanosphere can suppress the subversive expansion and shrinkage of crystal structure upon Na^+ insertion/extraction. Also, the morphology can reduce particles self-agglomeration and increase contact area between electrode and electrolyte.[65] The V_2O_5 hollow nanospheres finally demonstrated an excellent rate performance of 112.4 mAh g^{-1} at high current density of 640 mA g^{-1}. Even for the material with same component, the samples with different morphology might exhibit a diverse electrochemical properties. Li et al. synthesized $Na_3V_2(PO_4)_3$ with three different morphologies (irregular shaped, porous sponge-like and plate-like) by controlling the stoichiometric ratios of V_2O_5 and $H_2C_2O_4$ (Figure 6b.), and indicated that $Na_3V_2(PO_4)_3$ with porous sponge-like structure shows the best rate performance. For $Na_3V_2(PO_4)_3$ with porous sponge-like morphology, it provides a larger specific surface area and shorted diffusion distance of Na^+, thus significantly promoting the reaction kinetics of electrode material. Moreover, the unique porous sponge-like structure can withstand the strain generated by Na^+ deintercalation to keep the structure stable, especially at high current density, thus greatly improving the rate performance of cathode materials. an amazing electrochemical performances (101.77 mA h g^{-1} at 30 C and 89.28 mA h g^{-1} after 700 cycles) due to its highest surface area.[66]

3.5 Exposing active surface

Apart from controlling morphology, the modulation on exposed surface is also generally considered as an effective method to tune kinetic performance.[21,67–70] Yang et al. emphasized the significance of crystal surface on electrochemical performance because it is the channel through which Na^+ enter the bulk lattice from electrolyte.[71] Exposing active surface can increase area between effective Na ion diffusion channel and electrolyte, then to improve rate performance. He et al. prepared the distribution uniform $Na_{0.44}MnO_2$ cathode materials by a template-assisted sol-gel method (NSG-$Na_{0.44}MnO_2$), using acidic and reductive conditions to limit the growth of unfavorable birnessite phase in precursor.[43] Also, polystyrene was added to avoid morphology collapse and particle elongation during gel formation. The decomposition of polystyrene and citric acid during high-temperature combustion provides a reductive carbon-thermal condition, which not only inhibites the formation of 1D particles but also limites the induction of particles. Compared to SG-$Na_{0.44}MnO_2$ synthesized by conventional sol-gel method, the NSG-$Na_{0.44}MnO_2$ exhibit a strong grow tendency along [001] direction and a more uniform size distribution. The crystal growth of NSG-$Na_{0.44}MnO_2$ nanoplate particles is clearly presented in Figure 6c. Benefiting from the ingenious structure, NSG-$Na_{0.44}MnO_2$ could exhibit an outstanding rate performance. Similarly, Su et al. synthesized nanorod-like β-MnO_2 with exposed {111} crystal surface, which contributes to a rapid Na^+ diffusion during electrochemical test (capacity of 118 mAh g^{-1} at current density of 1600 mA g^{-1}.[21]

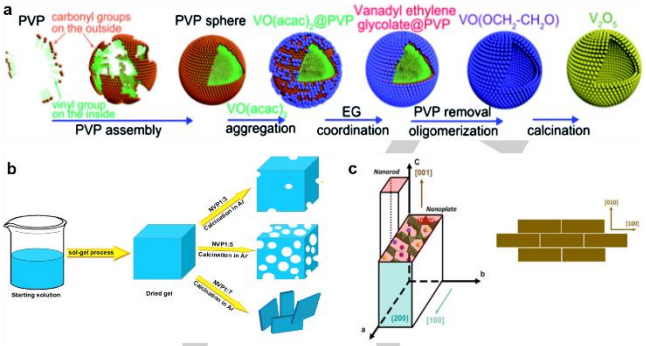

Figure 6. Schematic illustration for a) the evolution of V_2O_5 hollow nanospheres. Reproduced with permission.[65] Copyright 2014, Royal Society of Chemistry. b) the synthesis of $Na_3V_2(PO_4)_3$.[66] Reproduced with permission. Copyright 2016, Elsevier. c) crystal growth of NSG-$Na_{0.44}MnO_2$ nanorod and nanoplate. Reproduced with permission.[43] Copyright 2016, Elsevier.

3.6 Incorporating macromolecule

An open Na^+ diffusion path always responds to an excellent rate performance, which makes the strategy of incorporating macromolecule into the Na layer become an attractive method for designing high-rate performance compounds. Nam et al. synthesized $Na_{0.71}MnO_2{\cdot}0.25H_2O$ and indicated that the crystal water expands the layer spacing and weaken the binding energy between Na and O, leading to an enhanced rate performance.[72]

3.7 Combined strategies

Considering the respective advantage/shortcoming of each strategy mentioned above (the improved electrochemical activity and increased side reactions of nanocrystallization, the enhanced stability and lost capacities of surface coating), it is suggested to combine multi strategies with complementary characteristic with the aim of obtaining cathode materials with excellent rate performance.[23,52,73] For example, Jiang et al. developed $Na_3V_2(PO_4)_3$ (NVP)@C@CMK-3 through simple nanocasting technique. The reduction of NVP particles size has an effect of shortening the Na^+ diffusion length. In addition, the surface double carbon coating not only significantly enhance the electrical conductivity, but also reduce the self-aggregate phenomenon of nanoparticles.[74] The NVP@C@CMK-3 nanocomposite shows an excellent rate performance of 81 mAh g^{-1} at 30C. Similarly, Ramasamy et al. promoted rate performance of $Na_{0.5}Ni_{0.33}Mn_{0.67}O_2$ using a dual modification method (element doping and surface coating).[75] Cu was introduced to enhance the structural stability of $Na_{0.5}Ni_{0.33}Mn_{0.67}O_2$, which can reduce the damage of crystal structure during Na^+ insertion/extraction. Besides, the surface coating of MgO lower the side reaction between cathode and electrolyte, and suppress the phrase transition of P2-O2. The ingenious combination excellently improves its rate performance. Similarly, in order to enhance the rate performance of P2-type Na_xMnO_2 material, element doping and morphology optimization were often used simultaneously as a combined strategy. Nicolas Bucher et al. showed that the introduction of Co can effectively suppress the structural distortion

caused by Jahn-Teller effect of Mn^{3+}, optimize the Na^+/vacancy ordering, and improve the diffusion kinetics of Na ions. Meanwhile, benefiting from the hollow sphere structure of electrode materials, which can accommodate the volume changes during Na^+ deintercalation and increase the contact area between electrode and electrolyte, the best electrochemical properties of P2-type Na_xMnO_2 was obtained by combining the advantage of both strategies.[76]

4. Summary and Perspectives

In summary, we provide a systematic overview on influencing factors for poor rate performance of cathode materials in rechargeable NIBs and corresponding modifying strategies with various working mechanisms. Huge advances on designing cathode materials with excellent rate performances have been achieved, however, there are many challenges to further improving rate performances, especially how to better combine each strategy and balance their advantage and shortcoming. Therefore, there are a lot of space to design new materials or improve the kinetics of currently developed materials. We believe that more candidates will emerge as the cathode materials for NIBs, and the guidelines presented will prove an avenue for designing high-rate cathodes for next generation energy storage devices.

Acknowledgements

This work was supported by Basic Science Center Project of the National Natural Science Foundation of China under grant No. 51788104, the National Natural Science Foundation of China (Grant Nos. 21805038 and 51772301), the National Key R&D Program of China (Grant No. 2016YFA0202500), and the National Science Foundation of Fujian Province (2019J01284) and CAS.

Keywords: Na-ion batteries, cathode materials, rate performance, influencing factors, modifying strategies

Reference

[1] Y. Zhang, Y. Tang, W. Li, X. Chen, *ChemNanoMat* **2016**, *2*, 764–775.

[2] X. Wu, M. Sun, S. Guo, J. Qian, Y. Liu, Y. Cao, X. Ai, H. Yang, *ChemNanoMat* **2015**, *1*, 188–193.

[3] H. R. Yao, Y. You, Y. X. Yin, L. J. Wan, Y. G. Guo, *Phys. Chem. Chem. Phys.* **2016**, *18*, 9326–9333.

[4] V. Etacheri, R. Marom, R. Elazari, G. Salitra, D. Aurbach, *Energy Environ. Sci.* **2011**, *4*, 3243–3262.

[5] B. Scrosati, J. Hassoun, Y. K. Sun, *Energy Environ. Sci.* **2011**, *4*, 3287–3295.

[6] Y. Chen, J. Li, Y. Lai, J. Li, Z. Zhang, *ChemNanoMat* **2018**, *4*, 379–386.

[7] H. Pan, Y. S. Hu, L. Chen, *Energy Environ. Sci.* **2013**, *6*, 2338–2360.

[8] H. Kim, M. H. Lee, H. Kim, K. Kang, G. Yoon, K. Lim, Z. Ding, *Adv. Energy Mater.* **2016**, *6*, 1600943.

[9] M. D. Slater, D. Kim, E. Lee, C. S. Johnson, *Adv. Funct. Mater.* **2013**, *23*, 947–958.

[10] Q. Ni, Y. Bai, F. Wu, C. Wu, *Adv. Sci.* **2017**, *4*, DOI 10.1002/advs.201600275.

[11] Y. Lu, L. Wang, J. Cheng, J. B. Goodenough, *Chem. Commun.* **2012**, *48*, 6544–6546.

[12] P. F. Wang, Y. You, Y. X. Yin, Y. G. Guo, *J. Mater. Chem. A* **2016**, *4*, 17660–17664.

[13] Y. Jiang, Y. Yao, J. Shi, L. Zeng, L. Gu, Y. Yu, *ChemNanoMat* **2016**, *2*, 726–731.

[14] F. Sauvage, L. Laffont, J. M. Tarascon, E. Baudrin, *Inorg. Chem.* **2007**, *46*, 3289–3294.

[15] H. Yoshida, N. Yabuuchi, K. Kubota, I. Ikeuchi, A. Garsuch, M. Schulz-Dobrick, S. Komaba, *Chem. Commun.* **2014**, *50*, 3677–3680.

[16] S. M. Oh, S. T. Myung, J. Hassoun, B. Scrosati, Y. K. Sun, *Electrochem. commun.* **2012**, *22*, 149–152.

[17] H. Weng, G. Xu, H. Zhang, S. C. Zhang, X. Dai, Z. Fang, *Phys. Rev. B - Condens. Matter Mater. Phys.* **2011**, *84*, 3–6.

[18] C. J. Yu, S. H. Choe, G. C. Ri, S. C. Kim, H. S. Ryo, Y. J. Kim, *Phys. Rev. Appl.* **2017**, *8*, 1–9.

[19] L. Zhao, H. Zhao, Z. Du, N. Chen, X. Chang, Z. Zhang, F. Gao, A. Trenczek-Zajac, K. Świerczek, *Electrochim. Acta* **2018**, *282*, 510–519.

[20] Y. You, X. L. Wu, Y. X. Yin, Y. G. Guo, *Energy Environ. Sci.* **2014**, *7*, 1643–1647.

[21] D. Su, H. J. Ahn, G. Wang, *NPG Asia Mater.* **2013**, *5*, e70-7.

[22] Y. Liu, X. Fang, A. Zhang, C. Shen, Q. Liu, H. A. Enaya, C. Zhou, *Nano Energy* **2016**, *27*, 27–34.

[23] J. Qian, M. Zhou, Y. Cao, X. Ai, H. Yang, *Adv. Energy Mater.* **2012**, *2*, 410–414.

[24] C. Li, X. Miao, W. Chu, P. Wu, D. G. Tong, *J. Mater. Chem. A* **2015**, *3*, 8265–8271.

[25] J. Liu, K. Tang, K. Song, P. A. Van Aken, Y. Yu, J. Maier, *Nanoscale* **2014**, *6*, 5081–5086.

[26] X. Zhang, X. Rui, D. Chen, H. Tan, D. Yang, S. Huang, Y. Yu, *Nanoscale* **2019**, *11*, 2556–2576.

[27] W. Li, Z. Yao, Y. Zhong, C. Zhou, X. Wang, X. Xia, D. Xie, J. Wu, C. Gu, J. Tu, *J. Mater. Chem. A* **2019**, DOI 10.1039/C9TA02041A.

[28] P. Nie, L. Shen, G. Pang, Y. Zhu, G. Xu, Y. Qing, H. Dou, X. Zhang, *J. Mater. Chem. A* **2015**, *3*, 16590–16597.

[29] L. Li, P. Nie, Y. Chen, J. Wang, *J. Mater. Chem. A* **2019**, DOI 10.1039/C9TA01965K.

[30] M. J. Bierman, S. Jin, P. T. Anastas, *Energy Environ. Sci.* **2009**, DOI 10.1039/b912095e.

[31] W. Song, X. Ji, Z. Wu, Y. Zhu, Y. Yang, J. Chen, M. Jing, F. Li, C. E. Banks, *J. Mater. Chem. A* **2014**, *2*, 5358–5362.

[32] H. R. Yao, Y. X. Yin, Y. G. Guo, *Chinese Phys. B* **2015**, *25*, DOI 10.1088/1674-1056/25/1/018203.

[33] N. Yabuuchi, K. Kubota, M. Dahbi, S. Komaba, *Chem. Rev.* **2014**, *114*, 11636–11682.

[34] Y. Sun, S. Guo, H. Zhou, *Adv. Energy Mater.* **2018**, *1800212*, 1–18.

[35] P. Wang, H. Yao, X. Liu, Y. Yin, J. Zhang, Y. Wen, X. Yu, L. Gu, Y. Guo, **2018**, 1–10.

[36] S. Wang, C. Ma, Y. S. Meng, K. Nguyen, J. Alvarado, M. Kodur, *ACS Appl. Mater. Interfaces* **2017**, *9*, 26518–26530.

[37] X. Han, M. Xu, H. Lin, Q. Yuan, Y. Liu, B. Guo, Q. Fu, J. Yang, G. Liu, *Nanoscale* **2018**, *10*, 12625–12630.

[38] A. Konarov, Y.-K. Sun, H. Yashiro, S.-T. Myung, L. Shi, J. U. Choi, S. Yuan, J. H. Jo, *Adv. Funct. Mater.* **2018**, *28*, 1705968.

[39] P. F. Wang, Y. You, Y. X. Yin, Y. G. Guo, *Adv. Energy Mater.* **2018**, *8*, 1–23.

[40] L. Wang, Y. G. Sun, L. L. Hu, J. Y. Piao, J. Guo, A. Manthiram, J. Ma, A. M. Cao, *J. Mater. Chem. A* **2017**, *5*, 8752–8761.

[41] Y. Wang, G. Cao, *Adv. Mater.* **2008**, *20*, 2251–2269.

[42] M. D'Arienzo, R. Ruffo, R. Scotti, F. Morazzoni, C. M. Mari, S. Polizzi, *Phys. Chem. Chem. Phys.* **2012**, *14*, 5945–5952.

[43] X. He, J. Wang, B. Qiu, E. Paillard, C. Ma, X. Cao, H. Liu, M. C. Stan, H. Liu, T. Gallash, et al., *Nano Energy* **2016**, *27*, 602–610.

[44] Z. Jian, L. Zhao, H. Pan, Y. S. Hu, H. Li, W. Chen, L. Chen, *Electrochem. commun.* **2012**, *14*, 86–89.

[45] W. Li, L. Zeng, Y. Wu, Y. Yu, *Sci. China Mater.* **2016**, *59*, 287–321.

[46] W. K. Pang, H.-K. Liu, K. H. Seng, S. X. Dou, Z. Chen, S. Kalluri, Z. Guo, *ACS Appl. Mater. Interfaces* **2014**, *6*, 8953–8958.

[47] R. Klee, M. J. Aragón, R. Alcántara, J. L. Tirado, P. Lavela, *Eur. J. Inorg. Chem.* **2016**, *2016*, 3212–3218.

[48] K.-Y. Shen, M. Lengyel, L. Wang, R. L. Axelbaum, *MRS Commun.* **2017**, *7*, 74–77.

[49] Y. Cao, L. Xiao, W. Wang, D. Choi, Z. Nie, J. Yu, L. V. Saraf, Z. Yang, J. Liu, *Adv. Mater.* **2011**, *23*, 3155–3160.

[50] J. Z. Guo, X. L. Wu, F. Wan, J. Wang, X. H. Zhang, R. S. Wang, *Chem. - A Eur. J.* **2015**, *21*, 17371–17378.

[51] J. H. Shim, J. M. Han, J. H. Lee, S. Lee, *ACS Appl. Mater. Interfaces* **2016**, *8*, 12205–12210.

[52] X. Rui, W. Sun, C. Wu, Y. Yu, Q. Yan, *Adv. Mater.* **2015**, *27*, 6670–6676.

[53] W. J. Li, S. L. Chou, J. Z. Wang, J. L. Wang, Q. F. Gu, H. K. Liu, S. X. Dou, *Nano Energy* **2015**, *13*, 200–207.

[54] W. Duan, Z. Zhu, H. Li, Z. Hu, K. Zhang, F. Cheng, J. Chen, *J. Mater. Chem. A* **2014**, *2*, 8668–8675.

[55] H. R. Yao, P. F. Wang, Y. Gong, J. Zhang, X. Yu, L. Gu, C. Ouyang, Y. X. Yin, E. Hu, X. Q. Yang, et al., *J. Am. Chem. Soc.* **2017**, *139*, 8440–8443.

[56] H. R. Yao, P. F. Wang, Y. Wang, X. Yu, Y. X. Yin, Y. G. Guo, *Adv. Energy Mater.* **2017**, *7*, 1–6.

[57] P. F. Wang, H. R. Yao, X. Y. Liu, J. N. Zhang, L. Gu, X. Q. Yu, Y. X. Yin, Y. G. Guo, *Adv. Mater.* **2017**, *29*, 1–7.

[58] H. Li, X. Yu, Y. Bai, F. Wu, C. Wu, L. Y. Liu, X. Q. Yang, *J. Mater. Chem. A* **2015**, *3*, 9578–9586.

[59] L. Wang, Y. G. Sun, L. L. Hu, J. Y. Piao, J. Guo, A. Manthiram, J. Ma, A. M. Cao, *J. Mater. Chem. A* **2017**, *5*, 8752–8761.

[60] M. Matsui, F. Mizukoshi, N. Imanishi, *J. Power Sources* **2015**, *280*, 205–209.

[61] S. C. Han, H. Lim, J. Jeong, D. Ahn, W. B. Park, K. S. Sohn, M. Pyo, *J. Power Sources* **2015**, *277*, 9–16.

[62] S.-M. Oh, S.-T. Myung, J.-Y. Hwang, B. Scrosati, K. Amine, Y.-K. Sun, *Chem. Mater.* **2014**, *26*, 6165–6171.

[63] R. Yue, G. Gao, Y. Zhao, B. Wang, D. Tie, Q. Wang, F. Xia, R. Qi, *ACS Appl. Mater. Interfaces* **2019**, *11*, 6978–6985.

[64] Y. Wang, R. Xiao, L. Chen, M. Avdeev, Y.-S. Hu, *Nat. Commun.* **2015**, *6*, 1–9.

[65] D. W. Su, S. X. Dou, G. X. Wang, *J. Mater. Chem. A* **2014**, *2*, 11185–11194.

[66] H. Li, C. Wu, Y. Bai, F. Wu, M. Wang, *J. Power Sources* **2016**, *326*, 14–22.

[67] Y. Xiao, P. F. Wang, Y. X. Yin, Y. F. Zhu, X. Yang, X. D. Zhang, Y. Wang, X. D. Guo, B. H. Zhong, Y. G. Guo, *Adv. Energy Mater.* **2018**, *8*, 1–7.

[68] M. I. Jamesh, A. S. Prakash, *J. Power Sources* **2018**, *378*, 268–300.

[69] Y.-F. Zhu, Y.-B. Niu, Y. Xiao, J. Zhang, P.-F. Wang, X.-D. Guo, Y.-G. Guo, X.-D. Zhang, B.-H. Zhong, Y.-X. Yin, et al., *Adv. Mater.* **2018**, *30*, 1803765.

[70] G. Longoni, R. Lisette, P. Cabrera, S. Polizzi, D. A. Massimiliano, **n.d.**

[71] X. Yang, C. Wang, Y. Yang, Y. Zhang, X. Jia, J. Chen, X. Ji, *J. Mater. Chem. A* **2015**, *3*, 8800–8807.

[72] K. W. Nam, S. Kim, E. Yang, Y. Jung, E. Levi, D. Aurbach, J. W. Choi, *Chem. Mater.* **2015**, *27*, 3721–3725.

[73] W. Huang, J. Zhou, B. Li, L. An, P. Cui, W. Xia, L. Song, D. Xia, W. Chu, Z. Wu, *Small* **2015**, *11*, 2170–2176.

[74] Y. Jiang, Z. Yang, W. Li, L. Zeng, F. Pan, M. Wang, X. Wei, G. Hu, L. Gu, Y. Yu, *Adv. Energy Mater.* **2015**, *5*, 1402104.

[75] H. V. Ramasamy, K. Kaliyappan, R. Thangavel, V. Aravindan, K. Kang, D. U. Kim, Y. Park, X. Sun, Y. S. Lee, *J. Mater. Chem. A* **2017**, *5*, 8408–8415.

[76] N. Bucher, S. Hartung, J. B. Franklin, A. M. Wise, L. Y. Lim, H. Y. Chen, J. N. Weker, M. F. Toney, M. Srinivasan, *Chem. Mater.* **2016**, *28*, 2041–2051.

10.1002/cnma.201900254

WILEY-VCH

FOCUS REVIEW

FOCUS REVIEW

This review systematically summarizes the latest researches on exploiting high rate cathode materials for Na-ion batteries by optimizing composition and structure of materials. In addition, a comprehensive analysis on specific reasons hindering the kinetic performance is also discussed, expecting to deepen the understanding on mechanism behind rate performance and provide a new avenue of designing high performance cathode materials for Na-ion batteries.

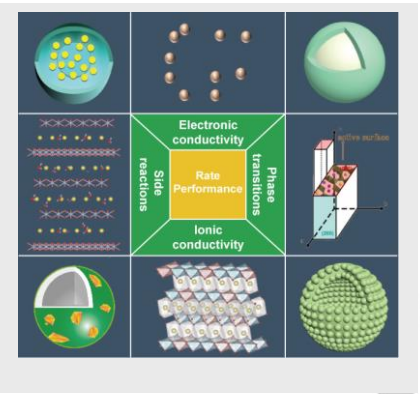

Wei-Jun Lv,[a],[c] Zhigao Huang,[a],[c] Ya-Xia Yin,[b],[d] Hu-Rong Yao,[a],[b],[c] Hai-Liang Zhu*[b] and Yu-Guo Guo*[b],[d]*

Page No. – Page No.

Strategies to Build High-Rate Cathode Materials for Na-Ion Batteries